Rigid-rod push–pull naphthalenediimide photosystems†

Naomi Sakai,[a] Adam L. Sisson,[a] Sheshanath Bhosale,‡[a] Alexandre Fürstenberg,[b] Natalie Banerji,[b] Eric Vauthey[b] and Stefan Matile*[a]

Received 4th June 2007, Accepted 28th June 2007
First published as an Advance Article on the web 16th July 2007
DOI: 10.1039/b708449h

Design, synthesis and evaluation of advanced rigid-rod π-stack photosystems with asymmetric scaffolds are reported. The influence of push–pull rods on self-organization, photoinduced charge separation and photosynthetic activity is investigated and turns out to be surprisingly small overall.

The design and synthesis of advanced optoelectric nanomaterials is a topic of current scientific interest.[1–18] In this report, we describe the synthesis and characteristics of push–pull *p*-octiphenyl **1**, a rigid-rod molecule that carries blue naphthalenediimides (*N*,*N*-NDIs) along the rigid-rod scaffold, a π-donating methoxy at one rod terminus and a π-accepting amide plus a negative charge at the other (Fig. 1). Compared to the previous photosystems **2** and **3**,[16–18] the new push–pull rod **1** contains a macrodipole along the rigid-rod scaffold. This axial macrodipole was of interest to explore the possibility of controlling photosynthetic and photophysical characteristics of **2** and **3** such as stabilization of the symmetry-breaking[2,16] photoinduced charge separation. These effects would be amplified with the *parallel* self-assembly of rod **1** into π-M-helix **4**. This supramolecule might form in lipid bilayers because of hindered translocation of the anionic carboxylate anchors across the membrane. In solution, dipole–dipole attraction should cause *antiparallel* self-assembly into quadruple π-M-helix **5** with reduced effects. These high expectations appeared meaningful considering the extensive evidence for remote control of optoelectric properties by α-helical macrodipoles. Highlights include fluorescence quenching in donor–acceptor dyads by α-helical dipoles,[19] amplified dark current along single α-helical dipoles,[20] and amplified photocurrents across monolayers of parallel α-helices on gold.[3] Moreover, rigid push–pull rods have been of use previously to create several variations of voltage-gated ion channels.[21,22]

The synthesis of rod **1** is summarized in Scheme 1. The *p*-sexiphenyl **6** was envisioned as an ideal building block to attach the π-attracting and π-donating rod termini **7** and **8**, respectively, and the blue *N*,*N*-NDIs **9** along the rigid-rod scaffold. Rapid access to *p*-sexiphenyl **6** from the commercially available biphenyl **10** and *tert*-butyl bromoacetate **11** has been reported previously.[22] Last year, we also synthesized *N*,*N*-NDI **9** starting with oxidation of pyrene **12**, reaction of the resulting dichlorodianhydride first with amines **13**, **14** and then with **15** to give **16**, followed by chemoselective removal of Alloc.[16]

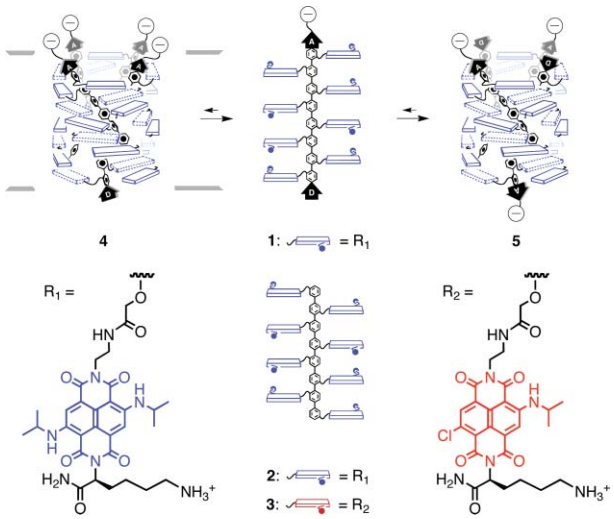

Fig. 1 Notional self-assembly of the blue, asymmetric push–pull rod **1** into parallel π-helix **4** in lipid bilayer membranes and antiparallel π-helix **5** in solution; for π-donor D and π-acceptor A with anionic anchor, please see Scheme 1. The symmetric blue and red controls **2** and **3** have been described.[18–20]

Rod terminus **7** was synthesized from benzaldehyde **17**, which was converted into iodinated compound **18** in four steps.[23] After acidic deprotection, benzaldehyde **19** was reacted first with *tert*-butyl bromoacetate **11**, followed by oxidation. Coupling of the resulting acid **20** with C-protected glycine **21** gave the desired π-accepting amide **22** with a protected carboxylate anchor. Pinacolboronate **23** was obtained by Pd-catalyzed conversion of aryl iodide **22**.[24] It was directly converted to the pull-fragment **7** with KHF_2 to benefit from increased stability, easier purification and higher reactivity of potassium trifluoroborates.[25–27]

The push-fragment **8** was synthesized from phenol **24**. The previously reported *ortho*-iodination gave pure regioisomer **25**,[28] which was subjected to Williamson ether synthesis with *tert*-butyl bromoacetate **11**. The obtained aryl iodide **26** was transformed *via* boronate **27** into the desired, air-stable and solid potassium trifluoroborate **8**.

Pull-fragment **7**, push-fragment **8** and chromophores **9** were coupled sequentially to *p*-sexiphenyl **6**. Suzuki coupling of *p*-sexiphenyl **6** first with push-fragment **8** gave *p*-septiphenyl **28** in 42% conversion yield, subsequent attachment of the pull-fragment **7** at the other terminus gave the final push–pull rod **29**. The lateral *tert*-butyl esters in **29** were cleaved with TFA without damage to the terminal benzyl esters. The liberated carboxylic acids along the rigid-rod scaffold of **30** were reacted with eight *N*,*N*-NDI amines

[a]*Department of Organic Chemistry, University of Geneva, Geneva, Switzerland. E-mail: stefan.matile@chiorg.unige.ch; Fax: (+41 22) 379 5123; Tel: (+41 22) 379 6523*
[b]*Department of Physical Chemistry, University of Geneva, Geneva, Switzerland*

† Electronic supplementary information (ESI) available: Experimental section. See DOI: 10.1039/b708449h

‡ *Current address:* Monash University, Clayton, Australia

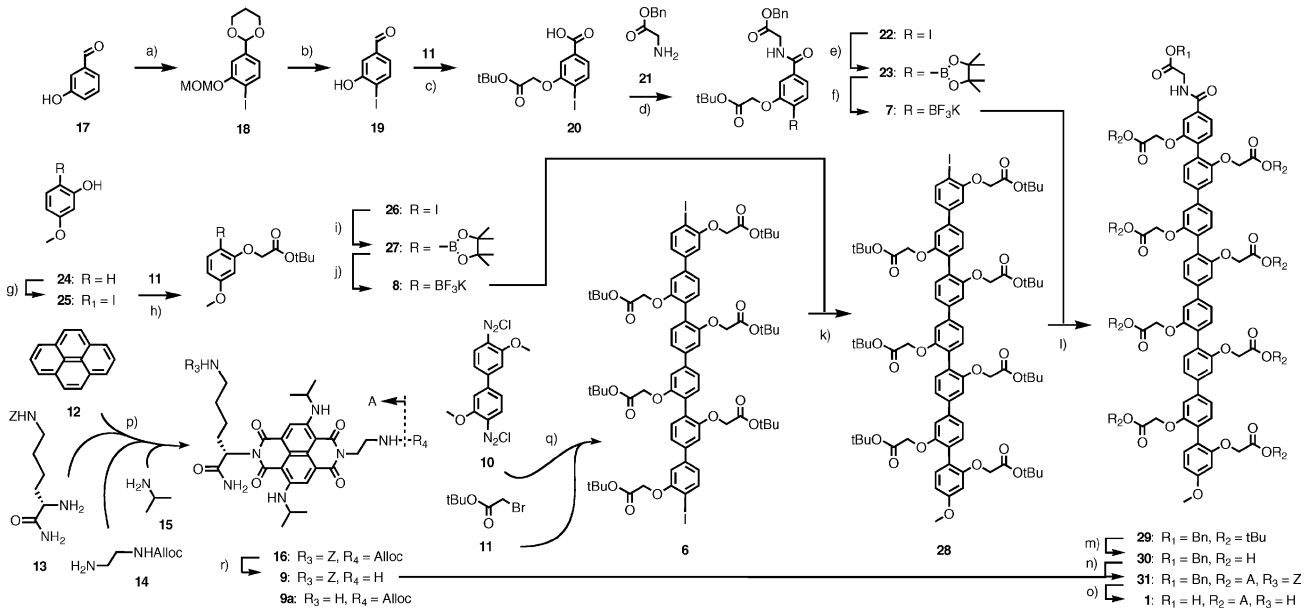

Scheme 1 (a) Four steps, see ref. 23. (b) HCl (aq), THF, 88%. (c) 1. Cs_2CO_3, DMF, 91%; 2. $NaClO_2$, NaH_2PO_4, H_2O_2, 91%. (d) HATU, iPr_2NEt, quant. (e) Pinacolborane, $PdCl_2$(dppf), Et_3N, CH_3CN, 1 h, reflux. (f) KHF_2, MeOH–H_2O, 2 h, rt, 47% from **22**. (g) AgOTf, I_2, $CHCl_3$.[27] (h) Cs_2CO_3, DMF, 92%. (i) Pinacolborane, $PdCl_2$(dppf), Et_3N, CH_3CN, 1 h, reflux, 88%. (j) KHF_2, MeOH–H_2O, 2 h, rt, quant. (k) $PdCl_2$(dppf), Et_3N, MeOH–THF 1 : 1, 30 min, reflux, 25%, conversion yield 42%. (l) $PdCl_2$(dppf), Et_3N, MeOH–THF 5 : 1, 30 min, reflux, 49%, conversion yield 66%. (m) TFA, CH_2Cl_2, 30 min, rt. (n) HATU, Et_3N, 2,6-di-*t*Bu-pyridine, DMF, rt, 24 h, 75% from **29**. (o) HBr, AcOH, TFA, thioanisole, pentamethylbenzene, 90 min, rt, quant. (p) Five steps, see ref. 22. (q) Four steps, see ref. 16. (r) Bu_3SnH, $Pd(PPh_3)_2Cl_2$, CH_2Cl_2, rt, 30 min, 86%, see ref. 16.

9, and the obtained conjugate **31** was fully deprotected with HBr–AcOH to give target molecule **1**.

The hypsochromic shoulder of the band around 600 nm in the absorption spectrum of the push–pull system **1** ↔ **5** was indicative of face-to-face π-stacking of the *N*,*N*-NDI chromophores.[2,16] The bisignate CD Cotton effect of this transition supported self-organization with *M*-helicity (Fig. 2C).[16,17] Strong in isopropanol, intermediate in methanol (MeOH) and weak in 2,2,2-trifluoroethanol (TFE), both effects exhibited identical solvent dependence (Fig. 2B). Unrelated to solvent polarity (Fig. 2A), this trend could reflect self-assembly of rod **1** into antiparallel π-helix **5** in isopropanol and MeOH but not as much in TFE.

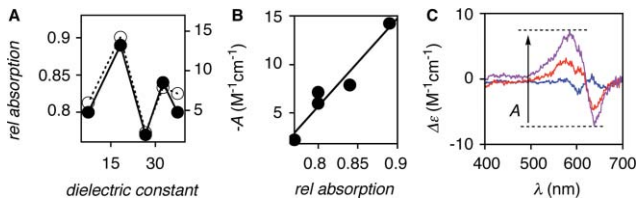

Fig. 2 Relative absorption of hypsochromic shoulder/absorption maximum in the absorption spectra (A, ●) and amplitude *A* in the CD spectra of **1** (A, ○) in, with decreasing dielectric constant, MeCN, MeOH (red), TFE (blue), isopropanol (purple) and THF. (C) Original CD spectra in isopropanol (purple), MeOH (red) and TFE (blue).

In MeOH, push–pull system **1** ($\Phi_{fl} = 4 \times 10^{-4}$) was 20-times less fluorescent than the symmetric control **2** ($\Phi_{fl} = 9 \times 10^{-3}$). The same weak emission was found for **1** in vesicles. This effect could imply more efficient photoinduced charge separation along the macrodipole in monomeric **1**. Alternatively, dipole–dipole attraction might promote antiparallel self-assembly, and increased charge separation might be the result of an increased concentration of π-stacked *N*,*N*-NDI chromophores in π-helix **5**. Moving from MeOH to TFE, the quantum yield of push–pull system **1** ($\Phi_{fl} = 3 \times 10^{-4}$) did not change significantly. This independence on partial disassembly of π-helix **5** into **1** suggested that indeed the macrodipole contributes to photoinduced charge separation in monomer **1**.

The early fluorescence dynamics were monitored using the fluorescence up-conversion technique (400 nm excitation, 100 fs pulses). In all cases, fluorescence decay was highly non-exponential, and at least 5 exponential functions were needed to reproduce the fluorescence decay. The average lifetime of push–pull system **1** (τ_{av} = 20–50 ps) was 4- (in MeOH) to 15-times (in TFE) shorter than that of the symmetric control **2** (τ_{av} = 200–310 ps). Particularly, the extent of ultrafast decay within the first 15 ps for push–pull system **1** (89% in MeOH, 76% in TFE) compared to **2** (66% in MeOH, 56% in TFE) could be interpreted as accelerated charge separation in push–pull photosystem **1** (Fig. 3A).

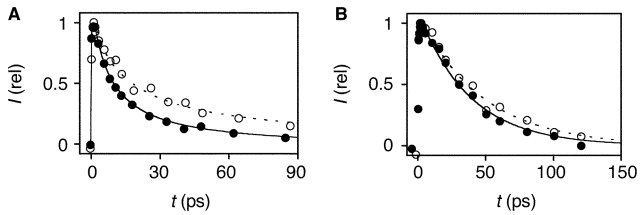

Fig. 3 Intensity-normalized time profiles of (A) fluorescence decay and (B) decay of the transient *N*,*N*-NDI$^{\bullet-}$ absorption of **1** (●) and **2** (○) in TFE. For full data sets, see ESI.†

The existence of photoinduced charge separation was confirmed by the transient absorption of the *N*,*N*-NDI$^{\bullet-}$ radical anion at 510 and above 670 nm following excitation with a 50 fs laser pulse at 610 nm.[16] According to the decay kinetics of the *N*,*N*-NDI$^{\bullet-}$ radical anion, the lifetime of the photoinduced charge-separated species of push–pull system **1** (MeOH: $\tau = 50$ ps, TFE: $\tau = 40$ ps, Fig. 3B) was quite similar to that of the blue control **2** (MeOH: $\tau =$ 65 ps,[16] TFE: $\tau = 50$ ps) but clearly, about 10-times shorter than that of the red control **3** (MeOH: $\tau \approx 500$ ps[18]). This suggested that, in contrast to accelerated charge separation, scaffold asymmetry in push–pull photosystem **1** did not affect charge recombination much.

The delivery of functional nanoarchitecture to bilayer membranes is an underrecognized and underexplored process that often determines the finally observed apparent activities.[29,30] For membrane delivery, concentrated solutions in various solvents (and eventual additives) are simply added to the vesicle suspension, and the functional compounds are hoped to reach the membrane before precipitation. To determine the solvent that best delivers photosystem **1**, large egg yolk phosphatidylcholine vesicles (EYPC LUVs) were labeled with *N*-(7-nitrobenz-2-oxa-1,3-diazol-4-yl)-1,2-dihexadecanoyl-*sn*-glycero-3-phosphoethanolamine (NBD-PE: λ_{ex} 463 nm, λ_{em} 535 nm). Quenching of lipid-bound NBD by FRET to *N*,*N*-NDIs indicates the relative quantity of delivered photosystem **1**. With the disassembling TFE as best (●) and the assembling MeOH as worst transporter (○), significant differences were found in the ability of solvent additives to deliver photosystem **1** to EYPC LUVs. Controls with monomeric *N*,*N*-NDIs **9a** (⊙)[16,18] confirmed that poor delivery by MeOH is compound-specific and not intrinsic (Fig. 4A).

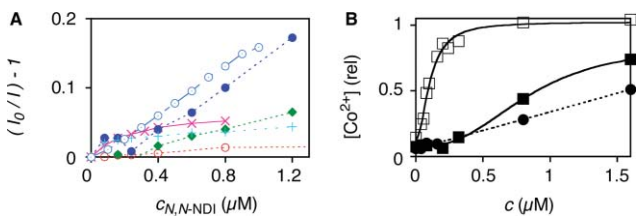

Fig. 4 Intensity-normalized concentration dependence for (A) membrane delivery and (B) photosynthetic activity of push–pull photosystem **1** (●), **2** (■) and **3** (□). (A) Relative emission *I* of NBD (λ_{ex} 463 nm, λ_{em} 535 nm) upon addition of **1** and monomeric *N*,*N*-NDI **9a**[16] (⊙) in TFE (●), DMSO (X), DMF (+), THF (♦) and MeOH (○,⊙) to NBD-PE-labeled EYPC LUVs. (B) Fractional reduction of $[Co(bpy)_3]^{3+}$ within EYPC LUVs with external EDTA after 15 min of irradiation of **1** (●), **2** (■) and **3** (□), all delivered with TFE.

The photosynthetic activity[13–18] of TFE-delivered push–pull photosystem **1** in EYPC LUVs was determined with the "Hurst assay".[15,18] In this assay, EDTA is used as an extravesicular sacrificial electron donor, and activity is detected optically at 320 nm as photoreduction of the intravesicular acceptor $[Co(bpy)_3]^{3+}$. Because EDTA oxidation is irreversible, the highest activity is found without membranes, a characteristic that allows for convenient assay calibration by lysis. Under these conditions, the photosynthetic activity of the push–pull photosystem **1** (●) was slightly weaker than that of the blue control **2** (■) and clearly weaker than with the red control **3** (□, Fig. 4B).[18] Interestingly, the Hill plot of the push–pull photosystem **1** ↔ **4** ↔ **5** exhibited no cooperativity under the present conditions.[17] Different to both symmetric controls, this finding suggested that the introduced asymmetry has a negative effect on the formation of active self-assembly. Facilitated antiparallel self-assembly into the hydrophobic π-helix **5** by dipole–dipole attraction before reaching the membrane could explain both poor activity and lack of cooperativity. Alternatively, these results could also be explained by hindrance of parallel self-assembly into **4** by dipole–dipole repulsion in the membrane. Moreover, vectorial control of partitioning by the terminal carboxylate might be lacking or opposite to expectations. Overall, we caution that a number of pathways to the functional system are conceivable to account for the reduced activity and cooperativity found with push–pull photosystems.

In summary, the introduction of asymmetry in photoactive rigid-rod π-stack nanoarchitecture is found to reduce fluorescence, to accelerate photoinduced charge separation, but to have little effect on charge recombination. These overall favorable properties, however, were not reflected in higher photosynthetic activity in lipid bilayer membranes. Hindered formation of the active suprastructure might account at least in part for these overall complex and surprisingly small effects. We conclude that vectorial self-assembly of asymmetric photosystems in lipid bilayers will be very challenging.

We thank D. Jeannerat, A. Pinto and S. Grass for NMR measurements, P. Perrottet, the group of F. Gülaçar and C. A. Schalley for MS measurements, H. Hagemann for access to the Xe lamp, one referee for helpful suggestions, and the Swiss NSF for financial support. S. B. is a fellow of the Roche Research Foundation.

Notes and references

1 N. S. Lewis, *Science*, 2007, **315**, 798–801.
2 M. R. Wasielewski, *J. Org. Chem.*, 2006, **71**, 5051–5066.
3 S. Yasutomi, T. Morita, Y. Imanishi and S. Kimura, *Science*, 2004, **304**, 1944–1947.
4 Supramolecular Dye Chemistry, *Topics in Current Chemistry*, ed. F. Würthner, Springer, Berlin, 2005, vol. 258.
5 V. Balzani, M. Venturi, A. Credi, *Molecular Devices and Machines*, Wiley-VCH, Weinheim, 2003, ch. 6.
6 S. Fukuzumi, *Bull. Chem. Soc. Jpn.*, 2006, **79**, 177–195.
7 D. M. Guldi, G. M. Rahman, F. Zerbetto and M. Prato, *Acc. Chem. Res.*, 2005, **38**, 871–878.
8 Y. Yamamoto, T. Fukushima, Y. Suna, N. Ishii, A. Saeki, S. Seki, S. Tagawa, M. Taniguchi, T. Kawai and T. Aida, *Science*, 2006, **314**, 1761–1764.
9 F. J. M. Hoeben, P. Jonkheijm, E. W. Meijer and A. P. H. J. Schenning, *Chem. Rev.*, 2005, **105**, 1491–1546.
10 M. Morisue, S. Yamatsu, N. Haruta and Y. Kobuke, *Chem.–Eur. J.*, 2005, **11**, 5563–5574.
11 L. Schmidt-Mende, A. Fechtenkotter, K. Müllen, E. Moons, R. H. Friend and J. D. MacKenzie, *Science*, 2001, **293**, 1119–1122.
12 G. Yu, J. Gao, J. C. Hummelen, F. Wudl and A. J. Heeger, *Science*, 1995, **270**, 1789–1791.
13 J. N. Robinson and D. J. Cole-Hamilton, *Chem. Soc. Rev.*, 1991, **20**, 49–94.
14 D. Gust, T. A. Moore and A. L. Moore, *Acc. Chem. Res.*, 2001, **34**, 40–48.
15 L. Zhu, R. F. Kairutdinov, J. L. Cape and J. K. Hurst, *J. Am. Chem. Soc.*, 2006, **128**, 825–835.
16 S. Bhosale, A. L. Sisson, P. Talukdar, A. Fürstenberg, N. Banerji, E. Vauthey, G. Bollot, J. Mareda, C. Röger, F. Würthner, N. Sakai and S. Matile, *Science*, 2006, **313**, 84–86.
17 S. Bhosale and S. Matile, *Chirality*, 2006, **18**, 849–856.
18 N. Sakai, A. L. Sisson, N. Banerji, A. Fürstenberg, E. Vauthey, S. Matile, submitted.

19 E. Galoppini and M. A. Fox, *J. Am. Chem. Soc.*, 1996, **118**, 2299–2300.
20 S. Sek, K. Swiatek and A. Misicka, *J. Phys. Chem. B*, 2005, **109**, 23121–23124.
21 N. Sakai, J. Mareda and S. Matile, *Acc. Chem. Res.*, 2005, **38**, 79–87.
22 N. Sakai, D. Gerard and S. Matile, *J. Am. Chem. Soc.*, 2001, **123**, 2517–2524.
23 M. R. Winke and R. C. Ronald, *J. Org. Chem.*, 1982, **47**, 2101–2108.
24 M. Murata, S. Watanabe and Y. Masuda, *J. Org. Chem.*, 1997, **62**, 6458–6459.
25 E. Vedejs, R. W. Chapman, S. C. Fields, S. Lin and M. R. Schrimpf, *J. Org. Chem.*, 1995, **60**, 3020–3027.
26 S. Darses, G. Michaud and J.-P. Genêt, *Eur. J. Org. Chem.*, 1999, 1875–1883.
27 G. A. Molander and B. Biolatto, *J. Org. Chem.*, 2003, **68**, 4302–4314.
28 M. Tsukayama, H. Utsumi, A. Kunugi and H. Nozaki, *Heterocycles*, 1997, **45**, 1131–1142.
29 L. M. Cameron, T. M. Fyles and C.-W. Hu, *J. Org. Chem.*, 2002, **67**, 1548–1553.
30 B. A. McNally, A. V. Koulov, B. D. Smith, J.-B. Joos and A. P. Davis, *Chem. Commun.*, 2005, **40**, 1087–1089.